(31) Flory, P. J. *Trans. Faraday Soc.* **1955**, *51*, 845.
(32) Otocka, E. P.; Roe, R. J.; Bair, H. E. *J. Polym. Sci., Polym. Phys. Ed.* **1974**, *12*, 1245.
(33) Mandelkern, L. "Crystallization of Polymers"; McGraw-Hill: New York, 1964.
(34) Strobl, G. R.; Hagedorn, W. *J. Polym. Sci., Polym. Phys. Ed.* **1978**, *16*, 1181.
(35) Jackson, J. F.; Mandelkern, L. "Analytical Calorimetry"; Johnson, J. F., Porter, R. S., Eds.; Plenum Press: New York, 1968; Vol. 1, p 1.
(36) Sakaguchi, F.; Maxfield, J.; Mandelkern, L. *J. Polym. Sci., Polym. Phys. Ed.* **1976**, *14*, 2137.
(37) Lauritzen, J. I., Jr. *J. Appl. Phys.* **1973**, *44*, 4353.
(38) Hillig, W. B. *Acta Metall.* **1966**, *14*, 1868.
(39) We thank Dr. I. Voigt-Martin for kindly supplying us with the electron micrographs.
(40) The previously reported SALS patterns for this series of quenched samples[10] indicates that the quenching temperature corresponded to about 70 °C.
(41) Our previous report[10] suffers from this deficiency, and the enthalpies of fusion are lower than the correct values. This error can be rectified, to a very good approximation, by adding 0.10 to the degree of crystallinities previously calculated from the enthalpy of fusion measurements.
(42) It should be noted that the premise of interface-controlled growth makes no assumption or imposes any requirements on the interfacial structure. In particular, identification with a regularly folded interface is unnecessary and incorrect.

Hydrophobic Domain Structure of Water-Soluble Block Copolymer. 1. Analysis of the Structure of the Polymolecular Micelle

Masahisa Ikemi,[1a] Nobuyuki Odagiri,[1a] Shinobu Tanaka,[1a] Isao Shinohara,*[1a] and Akio Chiba[1b]

Department of Polymer Chemistry and Department of Applied Physics, Waseda University, Ohkubo, Shinjuku-ku, Tokyo 160, Japan. *Received July 28, 1980*

ABSTRACT: Small-angle X-ray scattering and fluorometric measurements were carried out on an aqueous solution of the water-soluble ABA-type block copolymer of poly(2-hydroxyethyl methacrylate) (PHEMA) and poly(ethylene oxide) (PEO) to study micelle formation of the water-soluble block copolymer and its hydrophobic domain structure. The water-soluble block copolymer formed polymolecular micelles above ca. 0.1 g/dL and the hydrophobicity of the block copolymer was enhanced accompanied by intermolecular association. A spherical micelle model with a boundary region was proposed and a theoretical particle scattering function was derived for this model to compare with the experimental curve. The polymolecular micelle appeared to be constructed from a large number of molecules and the PHEMA core of the micelle was significantly large. The enhanced hydrophobicity is believed to result from aggregation of the PHEMA blocks within the interior core. The X-ray scattering data reveal that a large boundary region of the constituent blocks exists in the interfacial region between the core and the shell and that the ratio of half the boundary width to the core radius reached ca. 0.3. It is suggested that the hydrophobicity of the aggregated core is remarkably affected by intermixing of the constituent blocks.

Introduction

A water-soluble block copolymer composed of both hydrophobic and hydrophilic blocks is expected to possess characteristic properties,[2,3] and study of the structure and properties of such a block copolymer in water has attracted extensive attention. In particular, application to biomedical materials is of interest because the water-soluble block copolymer can completely restrict the aggregation and anticomplementary activity of human immunoglobulin.[3] The solution behavior of block copolymers in organic solvents has been studied,[4-9] but only a few papers have been published on water-soluble block copolymers.

Water-soluble amphiphilic polymers form hydrophobic regions effectively in water, due to the hydrophobic interaction between the nonpolar groups.[10-12] It has been suggested that the hydrophobic regions of polymers are affected, among other things, by factors such as the chemical structure of both the hydrophobic and the hydrophilic groups and their ratio in the copolymers.[13,14]

In a previous paper[2] we described the preparation of a water-soluble ABA-type block copolymer of hydrophobic poly(2-hydroxyethyl methacrylate) (PHEMA) and hydrophilic poly(ethylene oxide) (PEO) and discussed the hydrophobic region of the monomolecular block copolymer in dilute aqueous solution based on the results of fluorometric measurements with 8-anilinonaphthalene-1-sulfonate (ANS) as a fluorescent probe for hydrophobicity. The mode of arrangement of the constituent segments along the chain considerably affects the hydrophobic regions, and the block copolymer formed regions of strong hydrophobicity as compared with the corresponding random copolymer.

On the other hand, there is clear evidence of polymolecular micelle formation due to intermolecular association in the water-soluble ABA-type block copolymer described above. For the structure of intermolecular associates of block copolymers in organic solvents, a spherical micelle model has been proposed;[15-19] i.e., the aggregated insoluble chains are surrounded by the expanded soluble chains. Most of them are of the completely segregated type comprising two concentric spheres. It has been pointed out,[19] however, that considerable intermixing of the constituent blocks must take place for the solvent-swollen micelles in dilute solution.

We investigate in this article the structure and the hydrophobic regions of the intermolecular associates of the water-soluble block copolymer composed of hydrophobic PHEMA and hydrophilic PEO by means of small-angle X-ray scattering and fluorometric measurement using a fluorescent probe. A structural model for the intermolecular associate having an interfacial region between the core (PHEMA blocks) and the shell (PEO blocks) is proposed. The theoretical scattering functions are derived for this model and compared with the experimental results. The relation between the hydrophobic region and the

0024-9297/81/2214-0034$01.00/0

Table I
Preparation and Analysis of the HEMA-EO ABA-Type Block Copolymer

M_n of prepolymers				
amino-semi-telechelic oligo-HEMA[a]	hydroxyl-telechelic PEO[b]	% yield	HEMA mol fraction in block copolymer	
			found[c]	calcd[d]
1940	7210	69.8	0.104	0.153

[a] Value determined from amino group analysis. [b] Value determined from viscosity equation. [c] Value determined from hydroxyl group analysis. [d] Value calculated assuming ABA architecture.

structure of the polymolecular micelle is also discussed.

Experimental Section

Materials. The HEMA–EO ABA-type block copolymer was prepared by the same procedure as reported earlier,[2] so only brief details are given here. The amino-semitelechelic oligo-HEMA was prepared by radical telomerization of HEMA monomer, using 2-aminoethanethiol as a chain-transfer reagent. 2,4-Tolylene diisocyanate was introduced at both ends of PEO to obtain the isocyanato-telechelic PEO. The amino-semitelechelic oligo-HEMA was allowed to react with the isocyanato-telechelic PEO in DMF–chlorobenzene mixture at 0 °C for 48 h in order to obtain the HEMA–EO ABA-type block copolymer. The block copolymer obtained was purified by fractional precipitation based on the differential temperature dependence of solubility in ethylcellosolve between the block copolymer and the prepolymers. The results of the preparation of the sample are shown in Table I. The final product was completely soluble in water.

Fluorometric Analysis. Fluorometric measurements were carried out with a spectrofluorometer (Hitachi MPF 4). The fluorescence of ANS was excited by using incident light of 360 nm. Water from a thermostated bath was circulated through the jacket around the cell in order to maintain the sample at 30 ± 0.01 °C. Sufficient block copolymer was dissolved in an ANS solution of 1.0×10^{-5} mol/L to obtain a stock solution of 1.0 g/dL. The stock solution was diluted with an ANS solution of the same concentration to prepare samples of a given polymer concentration. Each sample was stored in a dark place until measurements were carried out.

Light Scattering. Light scattering measurements were carried out with a light scattering photometer (UNION GIKEN LS-601). The instrument was calibrated with benzene, for which the Rayleigh ratio is known. Measurement was made with light of 632.8 nm at 23 angles from 30 to 150°. The refractive index increment of the sample solution was determined by using a differential refractometer (UNION GIKEN RM-101). Distilled water was clarified by using filters of pore size 0.8 μm. A polymer solution of concentration 0.5 g/dL was centrifuged and transferred into light scattering cells with a ground-glass stopper just after the rotor came to rest. An aliquot of the stock solution was separated to determine the concentration by UV spectroscopy. Sufficient purified water was added directly to the light scattering cells containing the purified stock solution to obtain sample solutions of concentration ranging from 0.1 to 0.4 g/dL. The concentration of each solution was calculated from the weights of the solution and solvent. The volume change on mixing was neglected. The solution was stable and did not show any time-dependent change of light scattering.

Small-Angle X-Ray Scattering. Small-angle X-ray scattering (SAXS) measurement was carried out with a Rigaku Denki X-ray small-angle scattering apparatus using a Kratky slit. Copper radiation from an X-ray generator with a power of 35 kV and 26 mA was nickel-filtered and detected by a scintillation counter with a pulse-height analyzer. The incident X-ray source was collimated as described elsewhere.[20] Brass plates of 1-mm thickness having slits 30 mm × 5 mm were used as sample cells; both sides of the plates were covered with mica films of about 30-μm thickness as cell windows. The cell containing the sample solution was placed in a cell holder, around which water from a thermostated bath was circulated through the jacket to maintain the sample at 30 ± 0.01 °C. The temperature was measured by a thermocouple mounted in the cell holder near the area irradiated by the X-ray beam. The scattered intensity was measured at a fixed time of 2000 s from 0.16 to 0.04° by a step-scanning device with a step interval of 0.004°. Parasitic scattering from the slit system was negligible within the angular region in which measurements were carried out. The scattered intensity of the solvent was subtracted from that of the sample solution after correction for absorption.

Table II
Electron Density of Constituent Blocks of the Block Copolymer

constituent blocks	partial specific vol, cm³/mol	excess electron density, e/Å³
PHEMA	107.1	8.99×10^{-2}
PEO	37.1	5.69×10^{-2}

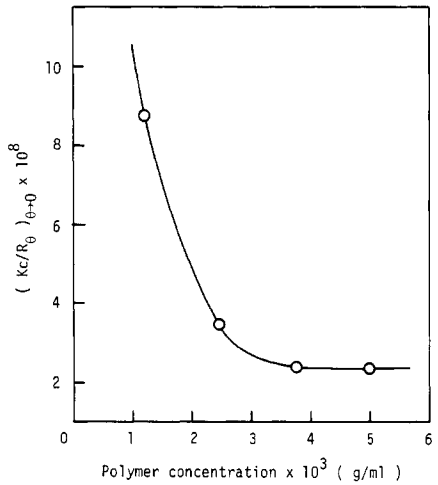

Figure 1. Plot of the reduced scattering intensity $(Kc/R_\theta)_{\theta\to 0}$ vs. polymer concentration for the HEMA–EO ABA-type block copolymer in water at 28.7 °C.

Electron Density. Density measurements were carried out with a digital precision densitometer (Anton Paar DMA 02C) at 30 ± 0.01 °C. The density of the aqueous solution of the PEO block was measured to determine the partial specific volume $\bar{v}$ of the PEO block in water. The $\bar{v}$ value of the PHEMA block could not be determined directly because it was insoluble in water. Therefore, the $\bar{v}$ value of the PHEMA block in water was evaluated from the $\bar{v}$ values of the block copolymer and the PEO block according to the relation[21] $v_t = x_A v_A + (1 - x_A)v_B$, where v_t is the specific volume of the block copolymer, v_A and v_B are the specific volumes of the A and B homopolymers, and x_A is the weight fraction of the A segments.

The values of electron density ρ for the constituent blocks were determined from $\rho = N/\bar{v}$, where N is a molar electron number. The results obtained are shown in Table II.

Results and Discussion

Intermolecular Association of the Water-Soluble Block Copolymer. Light scattering measurements were carried out on aqueous solutions of the HEMA–EO ABA-type block copolymer. The angular distribution of the scattered intensity was measured at five different concentrations and the reduced scattered intensity (Kc/R_θ) was extrapolated to zero angle. As shown in Figure 1, a plot of $(Kc/R_\theta)_{\theta\to 0}$ vs. polymer concentration deviated upward from linearity below a concentration of about 3.0×10^{-1} g/dL. The curvature of the plot indicates that the apparent molecular weight of the block copolymer increases with increasing polymer concentration in this concentration range, corresponding to a process of intermolecular association of the block copolymer.[18] Intermolecular association appeared to set in at least at a concentration of ca. 1.0×10^{-1} g/dL, although it was difficult to perform the experiment at lower concentration because

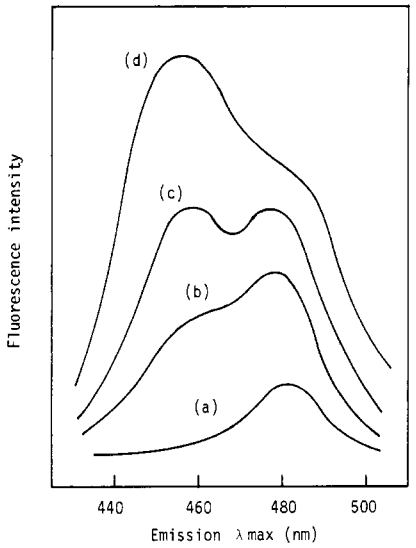

Figure 2. Fluorescence spectra for the aqueous solution of HEMA–EO block copolymer in the presence of ANS at 30 °C. [ANS] = 1.0×10^{-5} mol/L. [Polymer] (g/dL): (a) 1.0×10^{-2}, (b) 1.0×10^{-1}, (c) 2.0×10^{-1}, (d) 4.0×10^{-1}.

of the considerable decrease of scattered intensity. Nearly all the molecules of the block copolymer are believed to take part in the intermolecular association above a concentration of about 3.0×10^{-1} g/dL, since plots of $(Kc/R_\theta)_{\theta \to 0}$ vs. polymer concentration are linear.

Fluorometric measurements were carried out on aqueous solutions of the block copolymer in the presence of ANS in order to investigate the structural change of the hydrophobic domain accompanied by the intermolecular association. The ANS molecule, a fluorescent probe for hydrophobicity, is bound preferentially to the hydrophobic region of polymers, resulting in enhancement of the fluorescence quantum yield and a shift of the emission maximum (λ_{max}) toward shorter wavelength.[22-24] The fluorescence characteristics of ANS bound to the polymer chain should reflect the structure of the hydrophobic region. Figure 2 shows typical fluorescence spectra at different polymer concentrations for aqueous solutions of the block copolymer in the presence of ANS (1.0×10^{-5} mol/L). The emission λ_{max} of the fluorescence spectra is plotted against polymer concentration in Figure 3.

When an aqueous solution of PEO with ANS, i.e., one of the constituent blocks for the block copolymer, was excited with incident light of 360 nm, no fluorescence from ANS was observed even at high polymer concentration (data not shown), indicating that ANS does not bind to PEO chains. Therefore, the fluorescence spectra of ANS in block copolymer solutions are considered to reflect mainly the structure of the hydrophobic PHEMA domain.

In the concentration range below 1.0×10^{-3} g/dL, the emission λ_{max} of the block copolymer solution is nearly equal to that of the aqueous solution of ANS only, irrespective of the polymer concentration. The considerable blue shift of the emission λ_{max} with polymer concentration begins at about 1.0×10^{-3} g/dL and continues up to about 1.0×10^{-1} g/dL. At about 1.0×10^{-1} g/dL, a shoulder appears at shorter wavelength than λ_{max}. As shown in Figure 2, the peak of the shorter wavelength becomes predominant as polymer concentration is increased; the peak tends to shift slightly to shorter wavelength.

The appearance of the shoulder in the fluorescence spectra indicates that a more hydrophobic constituent is formed, coexisting with the monomolecular block copolymer. The polymer concentration at which the shoulder

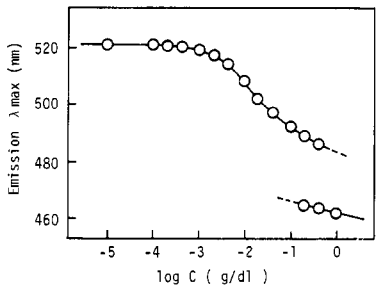

Figure 3. Polymer concentration dependence of the emission λ_{max} of the fluorescence spectra for aqueous solutions of the HEMA–EO block copolymer in the presence of ANS at 30 °C. [ANS] = 1.0×10^{-5} mol/L.

appears is approximately equal to the critical concentration for the intermolecular association of the block copolymer. These results show that an aggregated PHEMA domain with strong hydrophobicity was formed accompanied by intermolecular association of the block copolymer.

The distribution in hydrophobicity of the aggregated domain is believed to be relatively narrow since the fluorescence spectra of ANS in the shorter wavelength region resulting from the intermolecular associate was not so broad as shown in Figure 2. The peak around 450 nm dominated the peak near 480 nm as polymer concentration increased, indicating an increase in the ratio of the intermolecular association to the monomolecular block copolymer. The fact that the peak around 450 nm resulting from the intermolecular associate is slightly shifted toward shorter wavelength with increasing polymer concentration suggests either that the intermolecular associate became larger or that a change is taking place in the structure of the hydrophobic domain.

The hydrophobicity of the PHEMA domain of the monomolecular micelle appeared to be strongly dependent on polymer concentration even below the critical concentration for intermolecular association. This unusual concentration dependence of the emission λ_{max} suggests a change in the conformation of the monomolecular block copolymer prior to the formation of the polymolecular micelle.

Theoretical Interpretation for the Spherical Micelle Model. We assume the spherical micelle model with a boundary region resulting from a partial mixing of the constituent blocks. Figure 4 shows a schematic representation for this model. The distribution function of the excess electron density against water for both the constituent blocks of the block copolymer is also displayed in Figure 4.

Here, we consider a spherical micelle of total radius R. The PHEMA blocks form a spherical core of radius γR and the PEO blocks form the shell of the micelle, where γ ($0 < \gamma < 1$) is defined as the ratio of the core radius to the total radius R. The aggregated PHEMA chains are assumed to be uniformly distributed within the spherical core. The PEO chains obey random-flight statistics and are fully excluded from a hard core of radius γR. When the constituent blocks are completely segregated, AB junction points of the block copolymer are assumed to be on the spherical core surface of radius γR. When partial mixing of the constituent blocks takes place in the interfacial region between the core and the shell, AB chemical junction points on the core surface are assumed to be distributed. Thus, we assume that the junction points are distributed in the radial direction within the boundary of width $2\alpha\gamma R$ ($0 < \alpha < 1$) around the center γR according to the boundary function as defined later, where 2α is the ratio of the boundary width to the core radius γR.

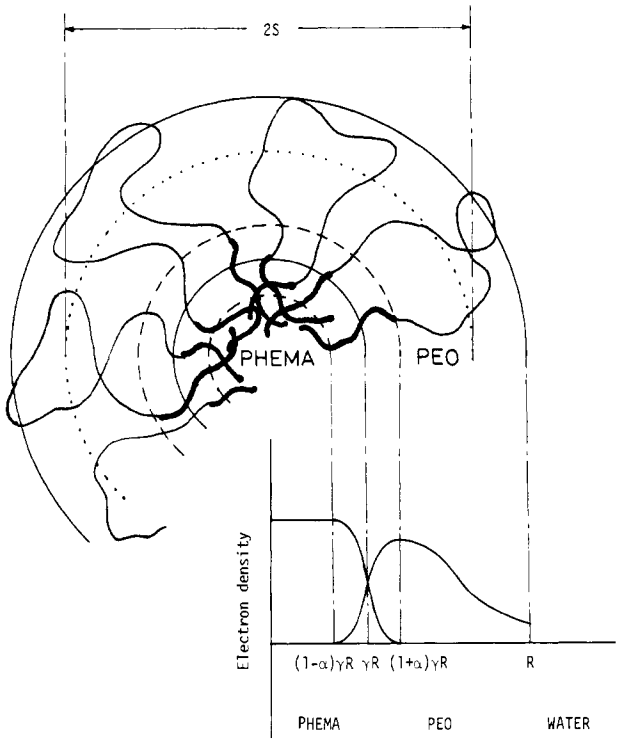

Figure 4. Schematic representation of the structure and electron density distribution for the polymolecular micelle of ABA-type block copolymers (see text).

The structure factor $F(h)$ for the block copolymer micelle was determined. In general, $F(h)$ is represented by

$$F(h) = \int_0^\infty \rho(r)\frac{\sin(hr)}{hr}4\pi r^2\,dr \quad (1)$$

where $\rho(r)$ represents a radial electron density distribution function, $h = (4\pi/\lambda)\sin(\theta/2)$ is the scattering vector, λ is the X-ray wavelength, θ is the scattering angle, and r is the distance from the center of the micelle.

In this micelle model, as shown in Figure 4, $\rho(r)$ is separated into ρ_c and ρ_s, which are the distribution functions for the electron density of the core and the shell, respectively. Both ρ_c and ρ_s are divided into two parts, i.e., the region consisting of a single component and the intermixing region, as expressed in the following equations:

$$\rho_c \begin{cases} \rho_1(r) = 1 \quad [0 < r < (1-\alpha)\gamma R] & (2) \\ \rho_2(r) = \frac{1}{2\pi}\left[-\sin\left(r-\gamma R\right)\frac{\pi}{\alpha\gamma R} - \left(r-\gamma R\right)\frac{\pi}{\alpha\gamma R} + \pi\right] & \\ \qquad [(1-\alpha)\gamma R < r < (1+\alpha)\gamma R] & (3) \end{cases}$$

$$\rho_s \begin{cases} \rho_3(r) = \frac{1}{2\pi}\left[\sin\left(r-\gamma R\right)\frac{\pi}{\alpha\gamma R} + \left(r-\gamma R\right)\frac{\pi}{\alpha\gamma R} + \pi\right] & \\ \qquad [(1-\alpha)\gamma R < r < (1+\alpha)\gamma R] & (4) \\ \rho_4(r) = \exp\left[-\left(\frac{r-(1+\alpha)\gamma R}{R-(1+\alpha)\gamma R}\right)^2\right] & \\ \qquad [(1+\alpha)\gamma R < r < R] & (5) \end{cases}$$

Because the aggregated PHEMA chains are assumed to be uniformly distributed within the core, the electron density is constant at any point. On the other hand, the PEO chains, which constitute the peripheral shell of the micelle, are excluded from the aggregated core and obey random-flight statistics. Consequently, when the constituent blocks are completely segregated ($\alpha = 0$), ρ_c and ρ_s are expressed by $\rho_1(r)$ and $\rho_4(r)$, respectively.

When partial mixing of the constituent blocks takes place, the chemical junctions of the block copolymer should distribute in the radial direction within the interfacial region centering the core radius. Here, the formation of the intermixing phase is regarded as the result of the distribution arising from the concentration gradient of the chemical junctions. Thus, the probability density distribution function $f(r)$ for the chemical junctions is derived from the diffusion equation as

$$f(r) = \exp\left[-\pi\left(\frac{r-\gamma R}{\alpha\gamma R}\right)^2\right] \Big/ \int_{(1-\alpha)\gamma R}^{(1+\alpha)\gamma R} \exp\left[-\pi\left(\frac{r-\gamma R}{\alpha\gamma R}\right)^2\right] dr \quad (6)$$

To express the statistical distribution of the junction points within the finite region of width $2\alpha\gamma R$ around the center γR, the boundary function is approximated by

$$f(r) = \cos^2\left(r-\gamma R\right)\frac{\pi}{2\alpha\gamma R} \Big/ \int_{(1-\alpha)\gamma R}^{(1+\alpha)\gamma R} \cos^2\left(r-\gamma R\right)\frac{\pi}{2\alpha\gamma R}\,dr \quad (7)$$

The distribution functions of the electron density for the constituent blocks within the boundary region are derived from the above equation and expressed by $\rho_2(r)$ and $\rho_3(r)$, respectively.

The electron density distribution functions for the core and the shell are normalized as

$$\rho_c^*(r) = \rho_c(r) \Big/ \int_0^{(1+\alpha)\gamma R} \rho_c(r)4\pi r^2\,dr \quad (8)$$

and

$$\rho_s^*(r) = \rho_s(r) \Big/ \int_{(1-\alpha)\gamma R}^{R} \rho_s(r)4\pi r^2\,dr \quad (9)$$

Thus, $F(h)$ is represented as

$$F(h) = N_c\int_0^{(1+\alpha)\gamma R} \rho_c^*(r)\frac{\sin(hr)}{hr}4\pi r^2\,dr + N_s\int_{(1-\alpha)\gamma R}^{R} \rho_s^*(r)\frac{\sin(hr)}{hr}4\pi r^2\,dr \quad (10)$$

where N_c and N_s are the total excess electron numbers of the core and shell, respectively.

The slit correction for the observed scattered intensity is required because line slit collimation was used in the small-angle X-ray scattering measurement. Since the experimental system is approximated by a system having infinite slit height, the scattered intensity $\tilde{I}$ is related to the true scattering intensity I by

$$\tilde{I}(h) = \int_{-\infty}^{\infty} W(u)I(u^2+h^2)^{1/2}\,du \quad (11)$$

where $W(u)$ is the effective slit-length weighting function. In this study, the theoretical scattering intensity I was smeared to compare the experimental curves. The weighting function was calculated for the collimation system used in this study by the method of Hendricks et al.[25]

The smeared theoretical particle scattering function $P(\theta)$ was derived from

$$P(\theta) = \tilde{I}(h)/\tilde{I}(0) \quad (12)$$

where $I(0)$ is the value for the case of $h = 0$ in eq 11.

A reciprocal particle scattering function $P(\theta)^{-1}$ is plotted in Figure 5 as functions of the structural parameters γ and α. The theoretical $P(\theta)^{-1}$ is dependent on both the parameters. The parameter γ causes a rapid upsweep of the $P(\theta)^{-1}$ plot in the lower angular region in comparison with

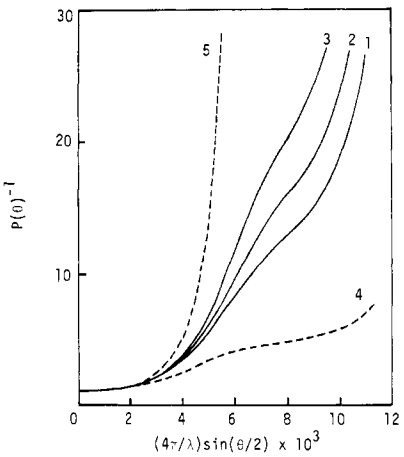

Figure 5. Reciprocal of the theoretical $P(\theta)$ for the spherical micelle model as a function of the structural parameters. $N_c/(N_c + N_s) = 0.346$, $S = 522$ Å. Solid lines are for $\gamma = 0.30$ with $\alpha = 0$ (curve 1), $\alpha = 0.4$ (curve 2), and $\alpha = 0.6$ (curve 3). Dashed lines and curve 1 are for $\alpha = 0$ with $\gamma = 0.20$ (curve 4), $\gamma = 0.30$ (curve 1), and $\gamma = 0.40$ (curve 5).

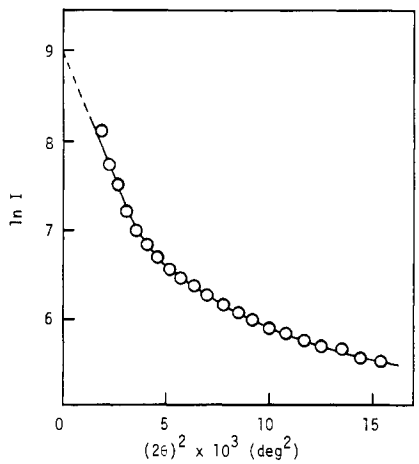

Figure 6. Guinier plot of the scattered intensity for the polymolecular micelle.

the parameter α. In the lower angular region, $P(\theta)^{-1}$ is solely dependent on the parameter γ, irrespective of the α values. Thus, the values of both parameters can be independently determined from the experimental curves.

Analysis of the Micelle Structure by Small-Angle X-Ray Scattering. The small-angle X-ray scattering measurements were carried out at 30 °C on an aqueous solution of the block copolymer (2.0 g/dL). This polymer concentration is far beyond the critical concentration for the intermolecular association of the block copolymer (see Figure 1). It should be noted that nearly all the molecules of the block copolymer take part in the polymolecular micelles and that the distribution in the size of the micelles is relatively narrow. Therefore, it is considered that scattering of the X-ray beam from the block copolymer solution is mainly due to the intermolecular associates and that the existence of the monomolecular micelle in the solution was negligible. The radius of gyration S was determined from[26]

$$I(\theta) = I_0 \exp[-(4\pi^2/3\lambda^2)S^2\theta^2] \quad (13)$$

where I_0 is the value of the scattered intensity extrapolated to zero angle. Figure 6 shows a Guinier plot of the scattered intensity for the polymolecular micelle.

We must evaluate the total radius R of the block copolymer micelle from the radius of gyration determined from the Guinier plot in order to compare the experimental scattering curve with the theoretical $P(\theta)$. The radius of gyration S of the block copolymer micelle for this model is related to the radius R by

$$S^2 = [k(\gamma,\alpha)]R^2 = N_c/(N_c + N_s)\int_0^{(1+\alpha)\gamma R} \rho_c^*(r)r^2 4\pi r^2\, dr + N_s/(N_c + N_s)\int_{(1-\alpha)\gamma R}^{R} \rho_s^*(r)r^2 4\pi r^2\, dr \quad (14)$$

where $k(\gamma,\alpha)$ is the proportionality constant between S^2 and R^2. The proportionality constant $k(\gamma,\alpha)$ is a function of the structural parameters γ and α. Therefore, the $k(\gamma,\alpha)$ values have to be determined for each pair of parameters from the integration of eq 14 by a numerical calculation. The values of the total radius R for each pair of parameters were determined from the $k(\gamma,\alpha)$ value and the experimental value of S^2.

If we employ an angular variable $(4\pi R/\lambda)\sin(\theta/2)$, the particle scattering functions are dependent solely on the shape of the scattering particles. In this case, however, the experimental curve is also a function of the structural parameters γ and α, since the angular variable with the total radius R $[=[1/k(\gamma,\alpha)]^{1/2}S]$ depends on the structural parameters. Therefore, to make it easy to compare with the theoretical curve, the observed intensity is plotted against the angular variable $(4\pi/\lambda)\sin(\theta/2)$, which is independent of the structural parameters.

Table III
Summary of SAXS Results on the Polymolecular Micelle for the HEMA-EO ABA-Type Block Copolymer in Water at 30 °C

characteristic	dimension
γ	0.33
α	0.30
radius of gyration (S), Å	591
total radius (R), Å	957
core radius (γR), Å	316
boundary width ($2\alpha\gamma R$), Å	189

Figure 7 shows a reciprocal plot of the experimental $P(\theta)$ in comparison with the theoretical $P(\theta)$ for the structural parameter $\alpha = 0$, i.e., for the case where no intermixing phase is formed and where the polymolecular micelle obeys the completely segregated model. In this case, the theoretical curve is a function of only the structural parameter γ. Agreement of the experimental curve with the theoretical $P(\theta)$ cannot be obtained, especially in the higher angular region. The deviation of the experimental curve from the theoretical $P(\theta)$ in the higher angular region indicates that the polymolecular micelle does not obey the completely segregated model, suggesting that the constituent unlike blocks interpenetrate to a certain extent in the interfacial region between the aggregated core and the peripheral shell. Consequently, the γ value for the polymolecular micelle was determined by fitting the experimental $P(\theta)^{-1}$ curve with the theoretical $P(\theta)^{-1}$ at lower scattered angles, where the theoretical $P(\theta)^{-1}$ depends mainly on the parameter γ.

In Figure 8, the experimental curve was compared with the theoretical $P(\theta)^{-1}$ in which the parameter γ determined in the lower angular region was kept constant ($\gamma = 0.33$). In this case, the theoretical curve is a function only of the structural parameter α, which represents the width of the intermixing phase. The good agreement of the experimental curve with the theoretical $P(\theta)^{-1}$ is observed over the entire range of scattered angle when $\alpha = 0.3$.

The values obtained for the parameters γ and α and the characteristics of the polymolecular micelle are shown in Table III. For the polymolecular micelle, the total micelle

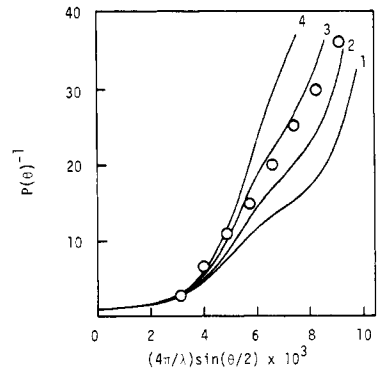

Figure 7. Comparison of the experimental curve with the theoretical $P(\theta)$ for the polymolecular micelle of the HEMA–EO block copolymer for $\alpha = 0$. $\gamma = 0.31$ (curve 1), 0.33 (curve 2), 0.35 (curve 3), and 0.37 (curve 4).

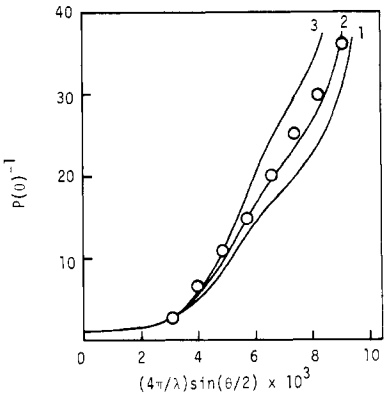

Figure 8. Comparison of the experimental curve with the theoretical $P(\theta)$ for the polymolecular micelle of the HEMA–EO block copolymer for $\gamma = 0.33$. $\alpha = 0$ (curve 1), 0.3 (curve 2), and 0.5 (curve 3).

radius is 954 Å and the value of γ is 0.33. The core radius of the micelle, which is determined from the parameter γ, reaches 315 Å. These values are considerably larger than those expected from the dimensions of the monomolecular block copolymer. This result shows that the polymolecular micelle is constructed from a large number of molecules of the block copolymer.

It should be noted that the extreme blue shift of the emission λ_{max} of ANS takes place simultaneously with the formation of the polymolecular micelle of the block copolymer as mentioned above. The blue shift of the emission λ_{max} implies an enhancement in hydrophobicity of the aggregated PHEMA domain as well as an increase in the amount of bound ANS. The result indicates that the internal structure of the PHEMA domain of the block copolymer changes with the formation of the polymolecular micelle. The SAXS experiment reveals that the polymolecular micelle is constructed from a large number of molecules and that a large domain of aggregated PHEMA blocks is formed. Therefore, the increase of the number participating in the PHEMA core is considered to be responsible for the change of the fluorescence spectra. The enhancement in hydrophobicity presumably occurs because the aggregation of a large number of the PHEMA chains results in the formation of a dense core from which water molecules are substantially excluded.

The SAXS data also reveals that the constituent different blocks interpenetrate each other, to a large extent, in the interfacial region between the aggregated core and the peripheral shell. The value of the parameter α is about 0.3 and the boundary width determined from the α value reaches 189 Å. It has been suggested[27-29] that in styrene–isoprene block copolymer films the domain boundary interface arises from a partial mixing of the incompatible segments and that the thickness of the boundary region is about 20 Å, independent of the molecular weight of the block copolymer. The value obtained for the polymolecular micelle in the aqueous solution is considerably larger than that expected for the bulk-phase system. Since PHEMA chains can hydrate a large amount of water molecules,[30] the aggregated core of the polymolecular micelle should swell somewhat in water. As a result, the PEO chains are considered to penetrate easily into the swollen core of the aggregated PHEMA chains, resulting in the formation of the intermixing phase between the swollen core and the peripheral shell of the soluble chains. The fact that a large intermixing phase exists in the interfacial region puts emphasis on the idea that the boundary region is an important factor in stabilizing the structure of the polymolecular micelle of the block copolymer. Our preliminary results suggest that the intermixing phase of the micelle decreases with increasing polymer concentration. Therefore, it is expected that the hydrophobicity of the aggregated core should be remarkably affected by intermixing of the constituent blocks. Demixing of the constituent blocks around the surface of the swollen core must result in the blue shift of the emission λ_{max} of ANS with increasing polymer concentration. Further detailed investigations are in progress.

References and Notes

(1) (a) Department of Polymer Chemistry. (b) Department of Applied Physics.
(2) Ikemi, M.; Odagiri, N.; Shinohara, I. *Polym. J.* **1980**, *12*, 777.
(3) Ikemi, M.; Watanabe, T.; Kigoshi, S.; Shinohara, I.; Tomono, T.; Suzuki, T.; Tokunaga, E., to be submitted for publication.
(4) Tanaka, T.; Kotaka, T.; Ban, K.; Inagaki, H. *Macromolecules* **1977**, *10*, 960.
(5) Tanaka, T.; Kotaka, T.; Inagaki, H. *Macromolecules* **1976**, *9*, 561.
(6) Birshtein, T. M.; Skvortsov, A. M.; Sariban, A. A. *Macromolecules* **1976**, *9*, 888.
(7) Han, C. C.; Mozar, B. *Macromolecules* **1977**, *10*, 44.
(8) Vitale, G. G.; LeGrand, D. G. *Macromolecules* **1976**, *9*, 749.
(9) Prud'homme, J.; Bywater, S. *Macromolecules* **1971**, *4*, 543.
(10) Anufrieva, E. V.; Birshtein, T. M.; Nekrasova, T. N.; Ptitsyn, O. B.; Sheveleva, T. V. *J. Polym. Sci., Part C* **1968**, *16*, 3519.
(11) Nekrasova, T. N.; Anufrieva, E. V.; Yel'yashevich, A. M.; Ptitsyn, O. B. *Vysokomol. Soedin.* **1965**, *7*, 913.
(12) Prokopova, E.; Stol, M.; Knizakoba, E.; Bohdanecky, M. *Makromol. Chem.* **1979**, *180*, 615.
(13) Okano, T.; Ikemi, M.; Shinohara, I. *Nippon Kagaku Kaishi* **1977**, 93.
(14) Okano, T.; Ikemi, M.; Shinohara, I. *Nippon Kagaku Kaishi* **1977**, 1702.
(15) Utiyama, H.; Takenaka, K.; Mizumori, M.; Fukuda, M.; Tsunashima, Y.; Kurata, M. *Macromolecules* **1974**, *7*, 515.
(16) Pleštil, J.; Baldrian, J. *Makromol. Chem.* **1973**, *174*, 183.
(17) Pleštil, J.; Baldrian, J. *Makromol. Chem.* **1975**, *176*, 1009.
(18) Price, C.; McAdam, J. D. G.; Lally, T. P.; Woods, D. *Polymer* **1974**, *15*, 228.
(19) Kotaka, T.; Tanaka, T.; Hattori, M.; Inagaki, H. *Macromolecules* **1978**, *11*, 138.
(20) Chiba, A.; Uzawa, S.; Usa, M.; Doi, S. *Rep. Prog. Polym. Phys. Jpn.* **1974**, *17*, 139.
(21) Glass, S. M.; Dole, M. *Macromolecules* **1979**, *12*, 965.
(22) Stryer, L. *J. Mol. Biol.* **1965**, *13*, 482.
(23) Wang, J. L.; Edelman, G. M. *J. Biol. Chem.* **1971**, *246*, 1185.
(24) Ghosh, S.; Basu, M. K.; Schweppe, J. S. *Biochim. Biophys. Acta* **1974**, *337*, 395.
(25) Hendricks, W.; Schmidt, P. W. *Acta Phys. Austriaca* **1967**, *26*, 97.
(26) Guinier, A.; Fournet, G. "Small Angle Scattering of X-Rays"; Wiley: New York, 1955.
(27) Hashimoto, T.; Nagatoshi, K.; Todo, A.; Hasegawa, H.; Kawai, H. *Macromolecules* **1974**, *7*, 364.
(28) Hashimoto, T.; Todo, A.; Itoi, H.; Kawai, H. *Macromolecules* **1977**, *10*, 377.
(29) Todo, A.; Uno, H.; Miyoshi, K.; Hashimoto, T.; Kawai, H. *Polym. Eng. Sci.* **1977**, *17*, 587.
(30) Refojo, M. F.; Yasuda, H. *J. Appl. Polym. Sci.* **1965**, *9*, 2425.